LA-5854-T
Thesis

0.3

UC-34c
Reporting Date: January 1975
Issued: February 1975

Pi–Meson Absorption on the Deuteron

by

Bruce Goplen*

*Present address: Science Applications, Inc.,
122 La Veta Drive NE, Albuquerque, NM 87108.

los alamos
scientific laboratory
of the University of California
LOS ALAMOS, NEW MEXICO 87544

An Affirmative Action/Equal Opportunity Employer

UNITED STATES
ATOMIC ENERGY COMMISSION
CONTRACT W-7405-ENG. 36

This report is derived from a dissertation submitted to the Department of Physics and Astronomy of The University of New Mexico, Albuquerque, NM, in partial fulfillment of the requirements for the Degree of Doctor of Philosophy in Physics. The report is the independent work of the author; it has not been edited by the Technical Information staff.

Work done in LASL Group MP-9 and partially supported by the AEC Division of Physical Research.

Printed in the United States of America. Available from
National Technical Information Service
U.S. Department of Commerce
5285 Port Royal Road
Springfield, VA 22151
Price: Printed Copy $7.60 Microfiche $2.25

CONTENTS

LIST OF FIGURES

LIST OF TABLES

PI-MESON ABSORPTION ON THE DEUTERON

Bruce Goplen, Ph.D.

The nonradiative absorption of positive pi-mesons by deuterons is studied within the framework of Lagrangian formalism and the impulse approximation. The pi-nucleon absorption interaction is taken to be pseudovector; however, the reaction is believed to be dominated by pi-nucleon scattering. Thus, the main thrust of the investigation is directed at three different approaches to the scattering interaction.

First, the Hamiltonian formalism of Koltun and Reitan is extended to include energetic pions. An off-shell form is chosen for p-wave scattering which at low energy reduces to the field-theoretical result of Klein. In the second approach, the S-matrix formalism of Lazard, Ballot and Becker is adapted for use with phenomenological nucleon-nucleon wave functions. Here the scattering interaction off-shell is given by the on-shell amplitudes. Finally, a pion optical model formalism is presented in which scattering graphs are included through modification of the external pion wave function. A new second-order optical model for the deuteron is given.

In all three approaches calculations are performed using phenomenological nuclear potentials, including the Boundary Condition Model and the Hamada-Johnston.

Calculated results for total and differential cross sections are compared with experimental data from 2 to 240 MeV pion kinetic energy.

The S-matrix approach and two forms of the Hamiltonian method are successful in representing the data, while the Kisslinger optical model produces a resonance below the experimental peak. Results are also presented for pi-deuteron elastic scattering calculations using the pion optical model, which gives reasonable agreement with the experimental data.

In conclusion, it does not appear possible to confirm the Galilean-invariant absorption term with this reaction. However, differential cross section results exhibit some sensitivity to nuclear models and to the D-state fraction in the deuteron. An experiment now under way at LAMPF may allow selection of preferred nuclear models. While use of an on-shell scattering Hamiltonian gives the desired total cross section, this result is not credible since calculations show great sensitivity to the off-shell behavior. The pi-deuteron absorption reaction offers a good means of measuring this off-shell behavior. Finally, a separable Hamiltonian interaction density is recommended for the investigation of nuclear structure using pi-meson absorption.

CHAPTER 1

INTRODUCTION

The absorption of pi-mesons on nuclei has proven a subject of considerable interest, both theoretical[1-49] and experimental.[50-73] Particularly important is the reaction leading to the emission of two nucleons, according to

$$\pi + A \rightarrow A^* + N + N \,. \tag{1-1}$$

The reason for interest in this reaction is that kinematical considerations indicate a sensitivity to the short-range nucleon-nucleon interaction. For example, in the nuclear absorption of a low-energy pi-meson, the outgoing nucleon(s) must have total kinetic energy roughly equal to the mass of the pion. The momentum required to make this reaction go cannot come from the low-energy pion, but must instead be found within the nucleus. This momentum is greater than that generally associated with Fermi momenta, so that single-nucleon emission is a relatively unlikely process. On the other hand, the required momentum may be produced by a correlated pair, and is associated with a very short-range interaction. Absorption of the pi-meson on the correlated pair then leads to two-nucleon emission, preferentially back-to-back, from the nucleus. This process may be represented by the equation,

$$\pi + N + N \rightarrow N + N \,. \tag{1-2}$$

Two-nucleon emission is thus, in principle, a reaction capable of testing the nuclear correlation function. The possible utility of the pi-meson in exploring nuclear structure was first suggested by Brueckner,[1] who noted the dominance of the reaction (1-1) and proposed the correlated pair hypothesis.

Of the general class of reactions (1-1), the process,

$$\pi^+ + d \rightarrow p + p, \qquad (1\text{-}3)$$

would seem to be of special interest, since it is more amenable to analysis than processes involving complicated nuclei. The solution of the deuteron two-body problem using Schrödinger's equation has been much studied, often in conjunction with nucleon-nucleon scattering. Thus both initial and final nuclear states in this reaction are relatively well known. Of particular importance is the absence in the final state of a residual nucleus, A*, which is believed to distort the outgoing nucleon-nucleon wave function.[35] Similarly, in the case of the deuteron there is no nuclear distortion of the incident pion wave function, except by the absorbing pair.

For these reasons it was hoped that a credible calculation could be performed for pion absorption on the deuteron. Without an adequate treatment of this process, one could not express confidence in the application of similar techniques for the extraction of nuclear structure information.

Much experimental data[62-72] is available for the absorption of pi-mesons on deuterons and the inverse reaction, production. These reactions can be related through detailed balance. Generally, we have emphasized the absorption cross section, σ_a, vs q, the incident pion momentum in the

overall-center-of-mass frame, or vs E_ℓ, the pion kinetic energy in the laboratory frame. The first choice tends to more clearly illustrate the q^{-1} behavior of the absorption cross section at low energy and to emphasize these data. After a minimum near 20 MeV, the total cross section appears to rise linearly with momentum to a prominent resonance which is centered near 140 MeV. The cross section then falls off rapidly just above the resonance.

The differential cross section is symmetric front-to-back in the overall-center-of-mass frame. In the low-energy region the angular distributions appear nearly isotropic, while near the resonance, distributions are strongly anisotropic with peaking in the forward and backward directions. In addition to total and differential cross sections, some polarization data are available. A recent experiment at CERN[72] has obtained differential cross sections at several higher energies. An experiment now under way at LAMPF[73] involves differential cross section measurements at pion energies between 10 and 60 MeV.

Early experiments involving the absorption reaction and its inverse helped to establish the spin and parity of the pi-meson. Consideration of parity conservation, conservation of angular momentum and nucleon-nucleon antisymmetry allow selection of final-state quantum numbers given the incident pion angular momentum. Table I presents allowed transitions for the first five partial waves in the expansion of the pion wave function. These transitions may be considered to occur from either the $^3S_1$ or the $^3D_1$ state of the deuteron.

The proton-proton states given in Table I describe coordinate-space distributions with respect to the relative momentum vector, $\vec{k}$. The

Table I

Allowed Transitions from the Deuteron $^3S_1$ and $^3D_1$ States

Pion Partial Wave	Proton-Proton State
s	$^3P_1$
p	$^1S_0$, $^1D_2$
d	$^3P_1$, $^3P_2$ - $^3F_2$, $^3F_3$
f	$^1D_2$, $^1G_4$
g	$^3F_3$, $^3F_4$ - $^3H_4$, $^3H_5$

experimental measurement, on the other hand, involves a distribution in θ, which is defined as the angle between the nuclear vector, $\overline{k}$, and the incident pion momentum vector, $\overline{q}$. It can be shown that this distribution carries components reflecting the incident pion partial wave. For example, the final state, $^3P_1$, resulting from the initial state, s-$^3S_1$, is isotropic in the overall-center-of-mass frame.

We now review some of the earlier theoretical treatments of this reaction. One of the first recorded is the work of Tamor,[40] who considered the decay of a mesic atom, which consists of a negative pi-meson bound to the deuteron by Coulomb forces. This work helped to establish the pi-meson as a pseudoscalar or pseudovector particle, that is, one of intrinsic negative parity. Another early calculation was that of Brueckner,[39] who calculated coefficients for the low-energy expression,

$$\sigma_a = A\bar{q}' + Bq. \qquad (1\text{-}4)$$

This form well represents the experimental absorption data below the resonance. Physical arguments suggest that the first term is representative of the pion s-wave, while the second is a p-wave term. As will be shown in Chapter 2, the production and absorption reactions can be related precisely by detailed balance. At low pion energy the production cross section is very nearly proportional to the absorption cross section times the pion momentum squared. Thus for production, the expression analogous to Eq. (1-4) contains terms which are linear and cubic in the pion momentum. Many of the early efforts sought to calculate one or both of these coefficients. The relativistic approach of D. Schiff,[46] for example, obtained reasonable agreement for the q^3 behavior on the low-energy side of the production resonance.

The majority of calculations, however, have been based upon Lagrangian formalism. Since the new calculations to be reported here fall into this category, a brief review is given of preceding efforts of this type. First, we wish to make clear the distinction between pi-nucleon operators and the pi-deuteron angular momentum, or partial wave. This problem arises since use is frequently made of the terms s-wave and p-wave in describing operators in the absorption Hamiltonian. These designations refer to the effect of the operator on the pion field. Thus a p-wave term contains a gradient operating on the pion field, while an s-wave term contains a gradient operating on the nucleon wave function. This latter term is also commonly referred to as the Galilean-invariant term. The words s-wave and p-wave are also used to refer to the form of the pi-nucleon scattering Hamiltonian. These, too, must be distinguished from pi-deuteron partial waves. Generally, the distinction will be clear from the context.

One of the earliest Lagrangian calculations was performed by Geffen,[41] who evaluated the differential cross section for the production reaction. Figure 1 shows a direct absorption graph for the production process.

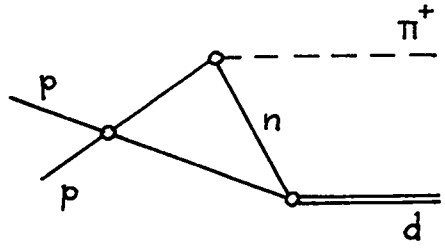

Fig. 1. Direct absorption graph for the production reaction.

Geffen calculated transition matrix elements of the form,

$$m = \langle \psi_f | T | \psi_i \rangle \,, \tag{1-5}$$

where ψ_f and ψ_i are nonrelativistic wave functions describing the final and initial two-nucleon states. The nuclear operator, T, was taken to be linear in the pseudoscalar pion field; s- and p-wave operator terms were successfully parameterized independently of energy. The initial nuclear states, $^3P_1$, $^1S_0$ and $^1D_2$, were obtained by solution of the Schrödinger equation using Jastrow potentials, while the deuteron wave function consisted of a combination of central and tensor Yukawa wells. Geffen obtained reasonable agreement with experimental data near threshold; his model suggested the importance of the nuclear interaction, in particular, a repulsive core, and inclusion of the D-state of the deuteron.

A similar calculation was performed by Lichtenberg,[42] who also calculated matrix elements using wave functions of physical nucleons. He considered a Hamiltonian linear in both pion field and pion momentum. The $^1S_0$ and $^1D_2$ states were then used to calculate the contribution to p-wave pions. The wave functions for the proton-proton states as well as those for the deuteron were obtained by solution of Schrödinger's equation using the Gartenhaus potential. This calculation gave qualitative agreement for the q^3 term in the production cross section near threshold.

In a later publication, Lichtenberg[43] demonstrated the role played by pi-nucleon scattering in the production reaction. In this calculation, a process was included in which the pi-meson, following production at the first nucleon, scatters off the second prior to emission. This matrix element thus included an integral over the intermediate-state momentum of an off-shell transition matrix for the (3,3) scattering state. The off-shell form was chosen to reduce on-shell to the free scattering amplitude. Results showed improved agreement with the q^3 experimental term. Lichtenberg also suggested the need for experiments near threshold to better determine the role of s-wave pions in this reaction.

Woodruff[44] performed a calculation for the production reaction near threshold in which both s- and p-wave scattering processes were included along with the direct production graph shown in Fig. 1. The scattering processes included forward and backward propagation in time, as illustrated by the graphs in Fig. 2. Meson production was considered to occur through the static p-wave term and an s-wave term chosen to make the production operator Galilean-invariant. Gartenhaus deuteron and Gammel-Thaler scattering wave functions were used. Woodruff found it possible to fit the low-energy experimental data with the exception of the pi-deuteron

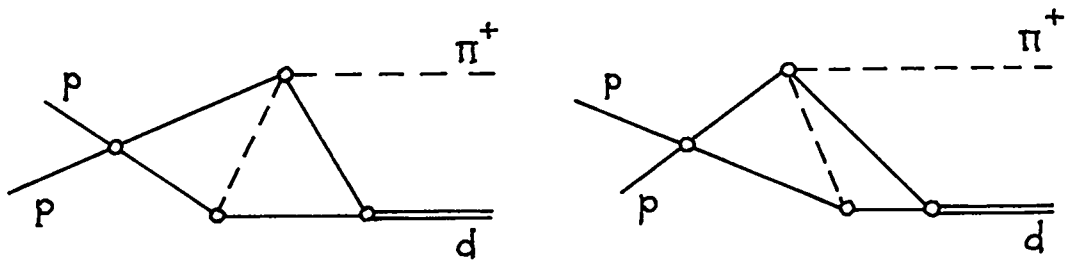

Fig. 2. Scattering graphs for the production reaction.

s-wave term. He pointed out that the Galilean-invariant contribution to this s-wave production was inadequate at threshold, due to cancellation of deuteron S- and D-state terms, but that s-wave pi-nucleon scattering (Fig. 2) could give a contribution of sufficient magnitude.

The general approach of Woodruff was also taken by Koltun and Reitan,[45] who obtained better agreement for the pion s-wave reaction. They considered specifically the absorption of a bound, negative pi-meson by the deuteron. Direct s-wave absorption as well as s-wave scattering on either nucleon followed by s- and p-wave absorption on the other were included. Their treatment differed from that of Woodruff mainly in the relative phase of the forward and backward terms involving propagation of the virtual meson. This factor and use of the Hamada-Johnston potential allowed better agreement with data at threshold. No important difference was found, however, when the Gammel-Thaler scattering wave functions and Gartenhaus deuteron were used. A significant contribution was obtained from the charge-exchange scattering term. Koltun and Reitan confirmed the approximate cancellation of the deuteron S- and D-state direct absorption graphs and thus demonstrated the dominance of scattering graphs even at low pion energies.

This bound-state calculation was later extended to include low-energy pions by Reitan,[48] who included s- and p-waves in the external pion wave function along with s- and p-wave scattering. New coupling constants were used in an attempt to gain agreement with the more recent low-energy data of Rose.[71]

Interest persists in the low-energy region. Cheon and Tohsaki[47] have performed a calculation similar in principle to that of Geffen, using Hamada-Johnston wave functions for the deuteron and an asymptotic form for the proton-proton $^3P_1$ wave function. They derived a form for the pi-nucleon scattering matrix assuming that the static approximation is applicable. Cheon and Tohsaki considered the basic absorption operator to be p-wave, and added to this an s-wave operator with a separate coupling constant as a free parameter. Their main objective was to determine the value of this coupling constant at low energy. They were not, however, able to achieve agreement with experiment using the usual theoretical reduction of the assumed pseudoscalar interaction. Instead, their parametric studies involving the separate coupling constant indicated close agreement with the earlier result of Geffen, who had considered only direct absorption.

A recent production calculation based on Lagrangian formalism has been done by Lazard, Ballot and Becker.[49] It is notable for the extent of agreement with experiment through the resonance region. The main feature of their S-matrix formalism is the inclusion of on-shell free scattering amplitudes directly in the matrix element. In their approximation I, Lazard et al. considered only s- and p-waves of the outgoing pion, and calculated Born terms and then corrections to these from proton-proton

scattering. In approximation II, the remaining proton-proton partial waves were added in Born approximation. Several deuteron pole models were used; proton-proton scattering was incorporated by modifying the irregular part of an asymptotic wave function with an exponential cutoff. By parameterizing this cutoff function, Lazard et al. attempted to consider the effects of variation in proton-proton short-range behavior. They found the final state interaction to affect the cross section significantly; similarly, sensitivity was found to the choice of deuteron wave function. They were able to compare angular distributions with the recent data from CERN, but were unable to achieve good agreement with the $\cos^4\theta$ behavior. Finally, they suggested that their calculation be redone with wave functions determined using phenomenological potentials.

We turn now to a brief discussion of the work to be presented here. The main points of interest in pi-deuteron absorption have been demonstrated to involve the nature of the absorption interaction, the nucleon-nucleon interactions, both initial and final, and the pi-nucleon scattering interaction. We generally neglect the question of the absorption interaction and assume the correct operator to be given by the non-relativistic reduction of the pseudovector interaction. Sensitivity to the nucleon-nucleon interactions is explored using realistic wave functions derived by solution of the Schrödinger equation. Phenomenological potentials used include the Hamada-Johnston and several cases of the Boundary Condition Model which represent different fractions of the deuteron D-state. However, the main thrust of this work focuses upon the nature of pi-nucleon scattering as reflected in the absorption reaction. Three separate approaches are taken to the absorption problem, each reflecting a different interpretation of pi-nucleon scattering.

In Chapter 2, the method of Koltun and Reitan is extended to include energetic pions. The p-wave scattering Hamiltonians are taken to be separable, off-shell forms which reduce at low energy to the field-theoretical results given by Klein. A free parameter in these forms reflects the pi-nucleon interaction distance. Still another p-wave Hamiltonian is created to correspond to the on-shell approximation.

In Chapter 3 we follow the suggestion of Lazard et al. and adapt their nuclear second-quantization approach to the more physical wave functions. At low energy these first two approaches will be seen to be nearly equivalent. However, important differences occur in the treatment of the p-wave scattering.

Finally, in Chapter 4 a somewhat different approach is offered in which terms nonlinear in the pion field are deleted from the Hamiltonian. Instead, we choose to modify the field in the remaining direct absorption terms by means of an optical model. Thus, the problem of pi-deuteron scattering is first solved using local, Laplacian and Kisslinger forms of the pion optical model. A new, second-order scattering formalism for the deuteron is offered and found to satisfactorily reproduce the elastic scattering data. With appropriate modification the resulting pion wave functions are used to replace the external pion field in the absorption problem. Direct and charge exchange processes are considered; however, the backwards propagation graphs and the spin-flip scattering terms are omitted.

Within the framework of each of these formalisms, we attempt to calculate the complete matrix element. Thus, all incident pion partial waves are included, and the treatment of the operators, angular momentum relations and integrals is without approximation, other than that

associated with numerical methods. Calculated results for total and differential cross sections are compared with experimental data from low energy through the resonance region. Chapter 5 summarizes the observations and conclusions.

CHAPTER 2

THE HAMILTONIAN FORMALISM

This work follows closely the theoretical approach of Koltun and Reitan,[45] who calculated the rate of absorption of a negative pion bound by Coulomb forces to the deuteron in an s-orbital. In their calculation, the Hamiltonian interaction density was evaluated between the initial pion state, $|n,s>$, and the final vacuum state, $|0>$. The resulting transition operator was then taken between initial and final nuclear states. Since only the pion s-orbital was considered, the $^3S_1$ and $^3D_1$ initial states contributed only to the $^3P_1$ final state.

We desire to extend this theory to include the absorption of energetic, positive pi-mesons by deuterons. It is therefore necessary to include higher pion partial waves; these will contribute to the final nuclear states previously given in Table I. The direct absorption p-wave operator must be retained, and, even for low incident pion energies, p-wave scattering terms must be added to the Hamiltonian. Several formulations of this scattering interaction are attempted.

Following the method of Koltun and Reitan, we calculate the nuclear transition operator,

$$T = \sum_{l=0}^{4} T^l,$$

where

$$T^0 = \langle 0 | \sum_{i=1}^{2} H_i^0 | \vec{q}, c=+1 \rangle$$

and

$$T^{\ell} = \langle 0 | \sum_{i \neq j} H_i^{\circ} (E - H + i\epsilon)^{-1} H_j^{\ell} | \vec{q}, c = +1 \rangle , \quad 1 \leq \ell \leq 4 .$$

(2-1)

Thus the Hamiltonian interaction density is evaluated between the final vacuum state and an initial state which contains a positive pion of momentum, q. T^{0} describes direct absorption while the four other transition operators include pi-nucleon scattering processes. In the scattering propagator, E is the total initial energy, while H is the total energy operator for the intermediate state.

These nuclear transition operators, T^{ℓ}, may be represented by graphs of the kind shown in Fig. 3. The first graph represents the direct absorption process, while the second and third reflect an intermediate pi-nucleon scattering. The third graph is included to permit the virtual meson to scatter backwards in time. The labels indicate particle identities for direct- and charge-exchange scattering processes.

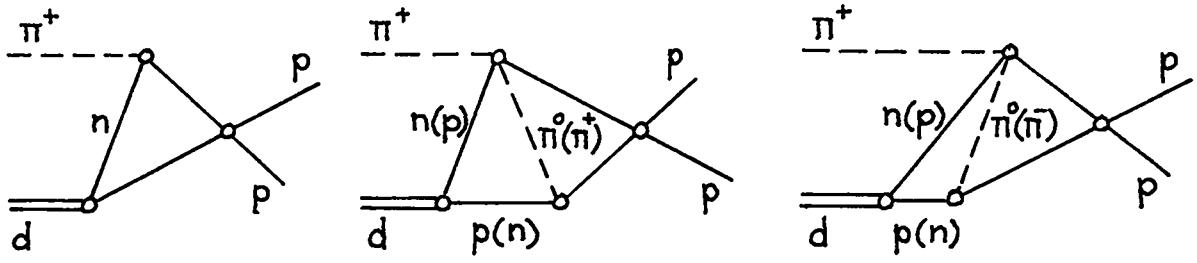

Fig. 3. Direct and scattering graphs for the absorption reaction.

The Hamiltonian interaction density for absorption is taken to be the nonrelativistic reduction of the pseudovector interaction, which is given by

$$H_j^0 = (4\pi)^{1/2} f \mu^{-1} i \bar{\sigma}_j \cdot \left\{ i \bar{q}_\pi \bar{\tau}_j \cdot \phi_j + (2M)^{-1} \left(\bar{P}_j \bar{\tau}_j \cdot \pi_j + \bar{\tau}_j \cdot \pi_j \bar{P}_j \right) \right\} . \tag{2-2}$$

In this equation, ϕ_j and π_j are the pion and conjugate fields, respectively, evaluated at the coordinate of the j^{th} nucleon. These fields couple with and are treated as vectors in isospin.

In this and subsequent chapters, subscripts are used to refer to the nucleon number, while superscripts describe vector components. Generally, use is made of tensor definitions in describing components of vector quantities; the exceptions to this are isospin and the pion field. σ_j, τ_j, χ_j and P_j refer, respectively, to the spin, isospin, spatial coordinate and momentum of the j^{th} nucleon. The symbol, q_π, represents the momentum operator on the pion field, while q, without sub- or superscript, refers to the external pion momentum. The prime superscript is used to designate intermediate-state meson and final-state nucleon variables. The zero subscript on a momentum variable denotes the zeroth component of four-momentum, or energy. All momenta are measured in the overall-center-of-mass frame. Finally, the symbols μ and M are used for the rest masses of the pion and nucleon, respectively. We do not distinguish the mass of the proton from that of the neutron.

The first term in Eq. (2-2) contains a p-wave operator on the pion field while the remaining terms are s-wave in character with respect to

the field. The sum of the s-wave terms is commonly referred to as the Galilean-invariant term. The operator ordering implies evaluation of nucleon momentum after and before absorption.

The coupling constant used in this and all subsequent chapters is the recently obtained value,[74] $f^2 = 0.077$. We point out that f occurs linearly in all matrix elements, and that the coupling constant may therefore be viewed as an overall normalization factor in the cross section.

The four remaining Hamiltonian terms describe pi-nucleon scattering. For the s-wave interaction, we have taken forms similar to those used by Koltun and Reitan. These are given by Klein[75] as

$$H_j^1 = 4\pi \lambda_1 \mu^{-1} \phi_j \cdot \phi_j$$

and

$$H_j^2 = 4\pi \lambda_2 \mu^{-2} \tau_j \cdot \phi_j \times \pi_j \quad . \tag{2-3}$$

The quantities, λ_i, are to be determined from the free scattering amplitudes and thus are energy-dependent. H^1 is a direct-exchange operator, while H^2 contains an isospin operator and thus includes charge-exchange terms.

It was suggested in Chapter 1 that the absorption peak is associated with the (3,3) scattering resonance. Therefore it would seem necessary to consider p-wave scattering. Klein has recommended the following p-wave Hamiltonian terms for use at low energy:

$$H_j^3 = -4\pi\lambda_3\mu^{-3}(\vec{q}_\pi\phi_j)\cdot(\vec{q}_\pi\phi_j)$$

and

$$H_j^4 = -4\pi\lambda_4\mu^{-3}\vec{\sigma}_j\tau_j\cdot(\vec{q}_\pi\phi_j)\times(\vec{q}_\pi\phi_j)\ . \qquad (2\text{-}4)$$

The dot-cross product in H^4 is understood to apply to the isospin-field operators as well as to the spin-momentum operators.

In calculating matrix elements for the scattering graphs, an integration is performed over all values of the intermediate pion momentum, $\vec{q}$. Thus it would seem desirable that the scattering Hamiltonian vanish in the off-shell high-momentum limit. A suitable form for the off-shell behavior has recently been suggested by several authors, including Landau and Tabakin,[76] Myhrer and Koltun,[77] and Eisenberg, Hüfner and Moniz.[78] We use this functional form to modify the Klein p-wave terms, according to

$$H_j^3 = -4\pi\lambda_3\mu^{-3}(\alpha^2+q^2)^2\left(\frac{\vec{q}_\pi}{\alpha^2+q_\pi^2}\phi_j\right)\cdot\left(\frac{\vec{q}_\pi}{\alpha^2+q_\pi^2}\phi_j\right)$$

and

$$H_j^4 = -4\pi\lambda_4\mu^{-3}(\alpha^2+q^2)^2\vec{\sigma}_j\tau_j\cdot\left(\frac{\vec{q}_\pi}{\alpha^2+q_\pi^2}\phi_j\right)\times\left(\frac{\vec{q}_\pi}{\alpha^2+q_\pi^2}\phi_j\right)\ . \qquad (2\text{-}5)$$

In these equations, α is a parameter which can be related to the pi-nucleon interaction distance. It will be treated here as a free

parameter. The expressions in Eq. (2-5) are seen to be equal in the limit as α goes to infinity to those of Eq. (2-4). They are also equal in the low-energy and low-momentum limit ($q << \alpha$ and $q_\pi << \alpha$) where Klein's results are assumed valid. The forms given in Eq. (2-5) correspond to a separable representation of the pi-nucleon T-matrix; therefore we shall refer to Eq. (2-5) as the separable Hamiltonian.

The nuclear transition operator described in Eq. (2-1) is calculated using the direct absorption, s-wave scattering and separable p-wave Hamiltonians given in Eqs. (2-2), (2-3) and (2-5). Details of this calculation are given in Appendix I. Before stating the result, we mention the desirability of working in center-of-mass and relative nuclear coordinates. The transition operator is then cast as a two-body operator. For coordinate space and momentum, the new variables may be obtained by the transformations,

$$\vec{X}_{1,2} = \vec{R} \pm \frac{1}{2}\vec{r}$$

and

$$\vec{P}_{1,2} = \frac{1}{2}\vec{K} \pm \vec{k} \,. \qquad (2\text{-}6)$$

In the overall-center-of-mass frame, the total final-state center-of-mass momentum, $\vec{K}$, must vanish. As demonstrated in Appendix I, use of this fact allows a reduction in the number of final integrals which must be evaluated. Treatment of the intermediate state is also discussed in this appendix. The five terms of the nuclear transition operator are given by

$$T^{0} = -(4\pi)^{1/2} f \mu^{-1} \sqrt{\frac{1}{2q_0}} \frac{1}{\sqrt{V}} e^{i\vec{q}\cdot\vec{R}}$$
$$\left\{ \left(e^{i\frac{\vec{q}\cdot\vec{r}}{2}} \tau_1^{+} \vec{\sigma}_1 + e^{-i\frac{\vec{q}\cdot\vec{r}}{2}} \tau_2^{+} \vec{\sigma}_2 \right) \cdot \left(1 + \frac{q_0}{2M} \right) \vec{q} \right.$$
$$\left. - \left(e^{i\frac{\vec{q}\cdot\vec{r}}{2}} \tau_1^{+} \vec{\sigma}_1 - e^{-i\frac{\vec{q}\cdot\vec{r}}{2}} \tau_2^{+} \vec{\sigma}_2 \right) \cdot \left(\frac{q_0}{M} \right) \vec{k}' \right\},$$

$$T^{1} = -\lambda_1 (4\pi)^{3/2} f \mu^{-2} \sqrt{\frac{1}{2q_0}} \frac{1}{\sqrt{V}} e^{i\vec{q}\cdot\vec{R}}$$
$$\left(e^{-i\frac{\vec{q}\cdot\vec{r}}{2}} \tau_1^{+} \vec{\sigma}_1 - e^{i\frac{\vec{q}\cdot\vec{r}}{2}} \tau_2^{+} \vec{\sigma}_2 \right) \cdot$$
$$\int \frac{d\vec{q}' \, e^{i\vec{q}'\cdot\vec{r}} \left\{ \left(2 + \frac{q_0}{2M} \right) \vec{q}' - \frac{q_0}{M} \vec{k}' \right\}}{(2\pi)^3 \left(\frac{q_0^2}{4} - q_0'^2 \right)},$$

$$T^{2} = -\lambda_2 (4\pi)^{3/2} f \mu^{-2} \sqrt{\frac{1}{2q_0}} \frac{1}{\sqrt{V}} e^{i\vec{q}\cdot\vec{R}}$$
$$\frac{3q_0}{4\mu} \left(\tau_1^{+} \tau_2^{3} - \tau_1^{3} \tau_2^{+} \right) \left(e^{-i\frac{\vec{q}\cdot\vec{r}}{2}} \vec{\sigma}_1 + e^{i\frac{\vec{q}\cdot\vec{r}}{2}} \vec{\sigma}_2 \right) \cdot$$
$$\int \frac{d\vec{q}' \, e^{i\vec{q}'\cdot\vec{r}} \left\{ \left(2 + \frac{q_0^2 + 2q_0'^2}{3q_0 M} \right) \vec{q}' - \frac{2(q_0^2 + 2q_0'^2)}{3q_0 M} \vec{k}' \right\}}{(2\pi)^3 \left(\frac{q_0^2}{4} - q_0'^2 \right)},$$

$$T^{3} = -\lambda_3 (4\pi)^{3/2} f \mu^{-4} \sqrt{\frac{1}{2q_0}} \frac{1}{\sqrt{V}} e^{i\vec{q}\cdot\vec{R}}$$
$$\left(e^{-i\frac{\vec{q}\cdot\vec{r}}{2}} \tau_1^{+} \vec{\sigma}_1 + e^{i\frac{\vec{q}\cdot\vec{r}}{2}} \tau_2^{+} \vec{\sigma}_2 \right) \cdot$$
$$\int \frac{d\vec{q}' (\alpha^2 + q^2) \, e^{i\vec{q}'\cdot\vec{r}} \left\{ \left(2 + \frac{q_0}{2M} \right) \vec{q}' - \frac{q_0}{M} \vec{k}' \right\} \vec{q}'\cdot\vec{q}}{(2\pi)^3 (\alpha^2 + q'^2) \left(\frac{q_0^2}{4} - q_0'^2 \right)}$$

and

$$T^4 = -\lambda_4 (4\pi)^{3/2} \int \mu^4 \sqrt{\frac{1}{2q_0}} \frac{1}{\sqrt{V}} e^{i\bar{q}\cdot\bar{R}}$$
$$(\lambda_1^+ \lambda_2^3 - \lambda_1^3 \lambda_2^+) \int \frac{d\bar{q}' (\alpha^2 + q^2) e^{i\bar{q}'\cdot\bar{r}}}{(2\pi)^3 (\alpha^2 + q'^2)\left(\frac{q_{b0}^2}{4} - q_{b0}'^2\right)}$$
$$\left\{ e^{-i\frac{\bar{q}\cdot\bar{r}}{2}} \bar{\sigma}_1 \cdot \left\{ \left(2 + \frac{q_0}{2M}\right)\bar{q}' - \frac{q_0}{M}\bar{k}' \right\} i\bar{\sigma}_2 \cdot \bar{q}' \times \bar{q} \right.$$
$$\left. - e^{i\frac{\bar{q}\cdot\bar{r}}{2}} \bar{\sigma}_2 \cdot \left\{ \left(2 + \frac{q_0}{2M}\right)\bar{q}' - \frac{q_0}{M}\bar{k}' \right\} i\bar{\sigma}_1 \cdot \bar{q}' \times \bar{q} \right\} . \qquad (2\text{-}7)$$

The nuclear wave functions used in these calculations are found from a solution of Schrödinger's equation using semiphenomenological nucleon-nucleon potentials. Included are the Hamada-Johnston potential and two cases of the Lomon-Feshbach Boundary Condition Model (BCM) which give different fractions of D-state in the deuteron. A description of the potentials as used in these calculations is given in Appendix II. The potentials include tensor coupling terms, and these lead to coupled, second-order differential equations. These equations are solved numerically using a three point, fifth-order differencing scheme which is developed in Appendix III.

The boundary conditions for the deuteron problem and two different techniques used to obtain eigenvalue solutions are presented in Appendix IV. The initial wave function for each orbital angular momentum state is written as

$$|\psi_i\rangle = (2\pi)^{-3/2} e^{i\bar{K}\cdot\bar{R}} \frac{u_L(r)}{r} |JMLSTM_T\rangle , \qquad (2\text{-}8)$$

where the angular momentum and isospin variables in the ket refer to the relative nucleon-nucleon system. These variables are, in the order given, total angular momentum and its projection, orbital angular momentum, spin, isospin and projection of isospin. For the deuteron, we have $J = S = 1$ and $T = M_T = 0$. Orbital angular momentum states include the S-state ($L = 0$) and the D-state ($L = 2$). The plane-wave factor describes the motion of the deuteron as an entity.

The proton-proton final state is dealt with in terms of its time-reversed equivalent, the scattering state. The boundary conditions for the tensor-coupled case are obtained using the eigenstate parameterization of Blatt and Biedenharn. This formalism along with symmetrization and time reversal requirements are developed in Appendix V. It will be noted that the final-state wave function is described in terms of helicity states. Thus, the outgoing relative momentum vector, $\bar{k}'$, becomes an important axis for integration and summing angular momentum components. As shown in Appendix V, a particular component of the final-state wave function may be written as

$$|\psi_f^-\rangle = (2\pi)^{-3/2} e^{i\bar{K}'\cdot\bar{R}} \, g^{M'}_{J'L'S'}(r) \, |J'M'L'S'T'M_T'\rangle , \tag{2-9}$$

where for the singlet and uncoupled-triplet states,

$$g^{M'}_{J'L'S'}(r) = \frac{2\sqrt{2\pi}}{k'} (2L'+1)^{1/2} i^{L'} e^{-i\delta_{L'}} \frac{u_{L'}(r)}{r} \begin{bmatrix} J'M' \\ L'0 \\ S'M' \end{bmatrix} , \tag{2-10}$$

and for the coupled states,

$$g^{M'}_{J'L'S'}(r) = (a\cos\epsilon_{J'} + b\sin\epsilon_{J'})e^{-i\alpha}\frac{u_{\alpha,J'\mp1}(r)}{r} - (a\sin\epsilon_{J'} - b\cos\epsilon_{J'})e^{-i\beta}\frac{u_{\beta,J'\mp1}(r)}{r} ,$$

where

$$a = \frac{2\sqrt{2\pi}}{k'}(2J'-1)^{1/2}\, i^{J'-1}\begin{bmatrix} J' & M' \\ J'-1 & 0 \\ S' & M' \end{bmatrix}$$

and

$$b = \frac{2\sqrt{2\pi}}{k'}(2J'+3)^{1/2}\, i^{J'+1}\begin{bmatrix} J' & M' \\ J'+1 & 0 \\ S' & M' \end{bmatrix} . \qquad (2\text{-}11)$$

The symbol,

$$\begin{bmatrix} J & M \\ L & M_L \\ S & M_S \end{bmatrix} ,$$

is a convenient notation for the Clebsch-Gordan coefficient; it may be idendified with the quantity $(L\ S\ J\ M \mid L\ M_L\ S\ M_S)$ defined by Edmonds.[79] The eigenstate symbols, α, β and $\epsilon_{J'}$, are discussed in Appendix V. For these calculations, the magnitude of the relative momentum vector is determined from energy conservation in the overall-center-of-mass frame. The protons are treated nonrelativistically.

The matrix element for the absorption reaction is obtained by evaluating the transition operator between final and initial nuclear states, according to

$$\mathcal{M} = \langle \bar{\psi}_f | T | \psi_i \rangle. \tag{2-12}$$

In this expression, the implied sums over the nuclear states include total and orbital angular momentum, but not spins or spin projections. Thus, for a given incident pion energy, the matrix element is a function of initial spin projection, final spin and its projection and θ, the angle between incident pion and either outgoing proton. The matrix element may be written explicitly as

$$\mathcal{M} = \sum_{\lambda=|M'-M|} C(S'M'M\lambda)\, Y^{*M'-M}_{\lambda}(\hat{k}', \hat{q}). \tag{2-13}$$

The form of Eq. (2-13) is motivated by results developed in Appendix VI and is chosen to provide the differential cross section with a functional dependence on the angle, θ. The symbol, λ, is used to denote the external pion partial wave.

Given a matrix element expressed in the form of Eq. (2-13), the differential cross section is obtained by averaging over the initial spin projection and summing over the final spin and its projection, according to

$$\frac{d\sigma_a}{d\Omega} = 2\pi \frac{q_o}{q} \frac{1}{3} \sum_{S'M'M} |\mathcal{M}|^2 \frac{V}{(2\pi)^3} \frac{M}{2} k'. \tag{2-14}$$

Since the momenta and the matrix element are determined in the overall-center-of-mass frame, the calculated differential cross section must be associated with this frame also. For historical reasons, it is usually expressed as a polynomial in cosθ-squared, thus directly reflecting the external pion partial waves entering the reaction. As shown in Appendix VII, Eq. (2-14) may be written as

$$\frac{d\sigma_a}{d\Omega} = \frac{MVk'q_2}{96\pi^3 q}\sum_{s'M'M}(-1)^{M'-M}\sum_{\lambda,\lambda'=|M'-M|}\sqrt{(2\lambda'+1)(2\lambda+1)}$$

$$C^*(s'M'M\lambda')\,C(s'M'M\lambda)\sum_{\ell=|\lambda'-\lambda|}^{\lambda'+\lambda}\begin{bmatrix}\ell & 0\\ \lambda' & 0\\ \lambda & 0\end{bmatrix}\begin{bmatrix}\ell & 0\\ \lambda' & M'-M\\ \lambda & M-M'\end{bmatrix}a_\ell^{-1}\sum_{n=0}^{\ell}d_\ell^{\,n}\cos^n(\theta)\,. \tag{2-15}$$

In this equation, a_ℓ and d_ℓ^n are coefficients which explicitly define the Legendre polynomials in terms of the cosine function. Equation (2-15) can be simplified to obtain the form,

$$\frac{d\sigma_a}{d\Omega} = \sum_{n=0} C_{2n}\cos^{2n}(\theta)\,. \tag{2-16}$$

Since the differential cross section expresses the probability for the arrival of either proton at the target, the total cross section must be given by

$$\sigma_a = \frac{1}{2}\int\frac{d\sigma_a}{d\Omega}\,d\Omega\,. \tag{2-17}$$

In practice, the cross section may be obtained directly from Eqs. (2-13) and (2-14) using the orthonormality of the spherical harmonics. The result is

$$\sigma_a = \frac{MVk'q_0}{48\pi^2 q} \sum_{\substack{S'M'M \\ \lambda=|M'-M|}} |C(S'M'M\lambda)|^2 . \qquad (2\text{-}18)$$

Alternately, the cosine-squared polynomial of Eq. (2-16) may be integrated to obtain

$$\sigma_a = 2\pi \sum_{n=0} \frac{C_{2n}}{2n+1} . \qquad (2\text{-}19)$$

The total cross section for the inverse reaction, or production, can be shown using detailed balance to be

$$\sigma_p = \frac{3}{2}\left(\frac{q}{k'}\right)^2 \sigma_a . \qquad (2\text{-}20)$$

We now return to the evaluation of the matrix element of Eq. (2-13) using results of Appendix VI. The integral over the center-of-mass coordinate, $\bar{R}$, yields only a delta function in momentum, according to

$$(2\pi)^{-3} \int d\bar{R}\, e^{-i\bar{K}'\cdot\bar{R}}\, e^{i\bar{K}\cdot\bar{R}}\, e^{i\bar{q}\cdot\bar{R}} = \delta(\bar{K}+\bar{q}-\bar{K}') . \qquad (2\text{-}21)$$

The matrix element is therefore determined solely by integration over the relative coordinate, $\bar{r}$. The complex coefficients are broken down into analytic angular integrals and one-dimensional radial integrals which must be performed numerically. These are labeled R_i and I_i, respectively. The result is that the coefficient may be written as

$$c(S'M'M\lambda) = i^{\lambda+l}(4\pi)^{3/2} f \bar{\mu}^{-1}\sqrt{\frac{1}{2q_0}}\frac{1}{\sqrt{V}}\sum_{J'L'L}\sum_{i=1}^{24} R_i I_i \ . \qquad (2\text{-}22)$$

The integrals, R_i and I_i, are functions of the initial and final nuclear quantum numbers as well as the incident pion partial wave. Thus, for each partial wave, these integrals must be evaluated for all possible interacting sets of initial and final two-nucleon states. These states have previously been listed in Table I.

The angular integrals, R_i, are given explicitly in Appendix VI and will not be repeated here since they are used in all three of the formalisms to be presented. These integrals were found to satisfy a Wigner-Eckart result on the Clebsch-Gordan coefficient involving conservation of total angular momentum,

$$\begin{bmatrix} J' & M' \\ J & M \\ \lambda & \mu \end{bmatrix} .$$

Thus, in practice, a momentum projection set involving a nonzero coupling coefficient was used to calculate integrals, R_i, and a reduced

matrix element. The Wigner-Eckart theorem[80] was then applied to obtain results for all other projections.

The derivation of the integrals, R_i, leads naturally to the following definitions for the one-dimensional radial integrals:

$$I_1 = -2\left(1+\frac{g_0}{2M}\right)\int dr\, r^2 \frac{u}{r}\, g'^*\left(\frac{d}{dr}-\frac{\lambda}{r}\right) j_\lambda ,$$

$$I_2 = -2\left(1+\frac{g_0}{2M}\right)\int dr\, r^2 \frac{u}{r}\, g'^*\left(\frac{d}{dr}+\frac{\lambda+1}{r}\right) j_\lambda ,$$

$$I_3 = -\frac{g_0}{M}\int dr\, r^2 \frac{u}{r}\, j_\lambda \left(\frac{d}{dr}-\frac{L'}{r}\right) g'^* ,$$

$$I_4 = -\frac{g_0}{M}\int dr\, r^2 \frac{u}{r}\, j_\lambda \left(\frac{d}{dr}+\frac{L'+1}{r}\right) g'^* ,$$

$$I_5 = \mu\left(\lambda_1+\frac{3g_0}{2\mu}\lambda_2\right)\left(2+\frac{g_0}{2M}\right)\int dr\, r^2 \frac{u}{r}\, f_{31}\, j_\lambda\, g'^* ,$$

$$I_6 = \mu\left(\lambda_1+\frac{3g_0}{2\mu}\lambda_2\right)\left(2+\frac{g_0}{2M}\right)\int dr\, r^2 \frac{u}{r}\, f_{31}\, j_\lambda\, g'^* ,$$

$$I_7 = -\left(\lambda_1+\frac{3g_0}{2\mu}\lambda_2\right)\frac{g_0}{M}\int dr\, r^2 \frac{u}{r}\, f_{20}\, j_\lambda \left(\frac{d}{dr}-\frac{L'}{r}\right) g'^* ,$$

$$I_8 = -\left(\lambda_1+\frac{3g_0}{2\mu}\lambda_2\right)\frac{g_0}{M}\int dr\, r^2 \frac{u}{r}\, f_{20}\, j_\lambda \left(\frac{d}{dr}+\frac{L'+1}{r}\right) g'^* ,$$

$$I_9 = -\lambda_3 q\left(2+\frac{g_0}{2M}\right)\int dr\, r^2 \frac{u}{r}\, \tilde{f}_{40}\, j_{\lambda-1}\, g'^* ,$$

$$I_{10} = -\lambda_3 q\left(2+\frac{g_0}{2M}\right)\int dr\, r^2 \frac{u}{r}\, \tilde{f}_{40}\, j_{\lambda+1}\, g'^* ,$$

$$I_{11} = -\lambda_3 q\left(2+\frac{g_0}{2M}\right)\int dr\, r^2 \frac{u}{r}\, \tilde{f}_{42}\, j_{\lambda-1}\, g'^* ,$$

$$I_{12} = -\lambda_3 q\left(2+\frac{g_0}{2M}\right)\int dr\, r^2 \frac{u}{r}\, \tilde{f}_{42}\, j_{\lambda+1}\, g'^* ,$$

$$I_{13} = \lambda_3 \frac{q}{\mu}\frac{q_0}{M}\int dr\, r^2 \frac{u}{r}\tilde{f}_{31} j_{\lambda-1}\left(\frac{d}{dr} - \frac{L'}{r}\right) g'^*,$$

$$I_{14} = \lambda_3 \frac{q}{\mu}\frac{q_0}{M}\int dr\, r^2 \frac{u}{r}\tilde{f}_{31} j_{\lambda-1}\left(\frac{d}{dr} + \frac{L'+1}{r}\right) g'^*,$$

$$I_{15} = \lambda_3 \frac{q}{\mu}\frac{q_0}{M}\int dr\, r^2 \frac{u}{r}\tilde{f}_{31} j_{\lambda+1}\left(\frac{d}{dr} - \frac{L'}{r}\right) g'^*,$$

$$I_{16} = \lambda_3 \frac{q}{\mu}\frac{q_0}{M}\int dr\, r^2 \frac{u}{r}\tilde{f}_{31} j_{\lambda+1}\left(\frac{d}{dr} + \frac{L'+1}{r}\right) g'^*,$$

$$I_{17} = -\lambda_4 2q\left(2 + \frac{q_0}{2M}\right)\int dr\, r^2 \frac{u}{r}\tilde{f}_{40} j_{\lambda-1}\, g'^*,$$

$$I_{18} = -\lambda_4 2q\left(2 + \frac{q_0}{2M}\right)\int dr\, r^2 \frac{u}{r}\tilde{f}_{40} j_{\lambda+1}\, g'^*,$$

$$I_{19} = -\lambda_4 2q\left(2 + \frac{q_0}{2M}\right)\int dr\, r^2 \frac{u}{r}\tilde{f}_{42} j_{\lambda-1}\, g'^*,$$

$$I_{20} = -\lambda_4 2q\left(2 + \frac{q_0}{2M}\right)\int dr\, r^2 \frac{u}{r}\tilde{f}_{42} j_{\lambda+1}\, g'^*,$$

$$I_{21} = \lambda_4 2\frac{q}{\mu}\frac{q_0}{M}\int dr\, r^2 \frac{u}{r}\tilde{f}_{31} j_{\lambda-1}\left(\frac{d}{dr} - \frac{L'}{r}\right) g'^*,$$

$$I_{22} = \lambda_4 2\frac{q}{\mu}\frac{q_0}{M}\int dr\, r^2 \frac{u}{r}\tilde{f}_{31} j_{\lambda-1}\left(\frac{d}{dr} + \frac{L'+1}{r}\right) g'^*,$$

$$I_{23} = \lambda_4 2\frac{q}{\mu}\frac{q_0}{M}\int dr\, r^2 \frac{u}{r}\tilde{f}_{31} j_{\lambda+1}\left(\frac{d}{dr} - \frac{L'}{r}\right) g'^*$$

and

$$I_{24} = \lambda_4 2\frac{q}{\mu}\frac{q_0}{M}\int dr\, r^2 \frac{u}{r}\tilde{f}_{31} j_{\lambda+1}\left(\frac{d}{dr} + \frac{L'+1}{r}\right) g'^*. \qquad (2\text{-}23)$$

The nature of each integral is easily ascertained from the preceding factor. The first four integrals result from direct absorption, while the next four represent s-wave scattering processes. The remaining

sixteen integrals represent absorption involving p-wave scattering processes. The initial- and final-state wave functions are written simply as u and g', respectively, all other arguments being omitted. The argument of the spherical Bessel function, j_λ, is $qr/2$. Although the result of the operator on j_λ in I_1 and I_2 is analytic, we have retained the operator form in preparation for the modified external pion wave function to be used in Chapter 4. The limits of integration over r are zero to infinity; in practice, the numerical integration was performed from the nucleon-nucleon core out to about 20 fermis.

The variables, $f_{n\ell}$ and $\tilde{f}_{n\ell}$, in the radial integrals represent integrals over intermediate pion momentum for s- and p-wave scattering, respectively. These intermediate integrals are defined by the general dimensionless forms,

$$f_{n\ell}(r) = -\mu'^{1-n}\,\frac{2}{\pi}\int_0^\infty \frac{dq'\,q'^{n}\,j_\ell(q'r)}{(q'^2+\mu'^2)}$$

and

$$\tilde{f}_{n\ell}(r) = -(\alpha^2+q^2)\,\mu'^{1-n}\,\frac{2}{\pi}\int_0^\infty \frac{dq'\,q'^{n}\,j_\ell(q'r)}{(q'^2+\mu'^2)(q'^2+\alpha^2)}\ ,$$

where

$$\mu'^2 = \frac{3\mu^2-q^2}{4}\ . \qquad (2\text{-}24)$$

The common factor in the denominators of $f_{n\ell}$ and $\tilde{f}_{n\ell}$ is simply the product of the forward and backward scattering propagators. Two s-wave intermediate integrals not in the form of Eq. (2-24) are recast in that form to allow grouping of similar terms. In particular, these integrals are

$$-\mu^{-1}\,\frac{2}{\pi}\int \frac{dq'\,q'^{2}\,j_0(q'r)\left(1+\frac{2q_0'^{2}}{q_0^{2}}\right)}{(q'^{2}+\mu'^{2})} \;=\; \frac{3}{2}\,f_{20}(r)$$

and

$$-\mu^{-2}\,\frac{2}{\pi}\int \frac{dq'\,q'^{3}\,j_1(q'r)\left(2+\frac{q_0}{3M}+\frac{2q_0'^{2}}{3q_0M}\right)}{(q'^{2}+\mu'^{2})} \;=\; \left(2+\frac{q_0}{2M}\right)f_{31}(r)\,. \tag{2-25}$$

For pion kinetic energies below roughly 180 MeV in the laboratory frame we have $q^2 < 3\mu^2$, or $\mu'^2 > 0$. In this case, and for $n + \ell$ odd, the intermediate integrals are unambiguously obtained by contour integration. The results are

$$f_{n\ell}(r) = -i^{n}\left(\frac{\mu'}{\mu}\right)^{n-1}\frac{1}{2}\left\{h_\ell^{1}(i\mu' r)+(-1)^{n}h_\ell^{2}(-i\mu' r)\right\}$$

and

$$\tilde{f}_{n\ell}(r) = -\left(\frac{\alpha^2+q^2}{\alpha^2-\mu'^2}\right)\left\{ i^n\left(\frac{\mu'}{\mu}\right)^{n-1}\frac{1}{2}\left\{ h_\ell^1(i\mu' r) + (-1)^n h_\ell^2(-i\mu' r)\right\}\right.$$

$$\left. - i^n\left(\frac{\alpha}{\mu}\right)^{n-1}\frac{1}{2}\left\{ h_\ell^1(i\alpha r) + (-1)^n h_\ell^2(-i\alpha r)\right\}\right\}. \tag{2-26}$$

The required integrals are given more explicitly by

$$f_{20}(r) = -\left(\frac{\mu'}{\mu}\right)\frac{e^{-\mu' r}}{\mu' r},$$

$$f_{31}(r) = -\left(\frac{\mu'}{\mu}\right)^2\left(1+\frac{1}{\mu' r}\right)\frac{e^{-\mu' r}}{\mu' r},$$

$$\tilde{f}_{31}(r) = -\left(\frac{\alpha^2+q^2}{\alpha^2-\mu'^2}\right)\left\{\left(\frac{\mu'}{\mu}\right)^2\left(1+\frac{1}{\mu' r}\right)\frac{e^{-\mu' r}}{\mu' r} - \left(\frac{\alpha}{\mu}\right)^2\left(1+\frac{1}{\alpha r}\right)\frac{e^{-\alpha r}}{\alpha r}\right\},$$

$$\tilde{f}_{40}(r) = \left(\frac{\alpha^2+q^2}{\alpha^2-\mu'^2}\right)\left\{\left(\frac{\mu'}{\mu}\right)^3\frac{e^{-\mu' r}}{\mu' r} - \left(\frac{\alpha}{\mu}\right)^3\frac{e^{-\alpha r}}{\alpha r}\right\}$$

and

$$\tilde{f}_{42}(r) = -\left(\frac{\alpha^2+q^2}{\alpha^2-\mu'^2}\right)$$

$$\left\{\left(\frac{\mu'}{\mu}\right)^3\left(1+\frac{3}{\mu' r}+\frac{3}{(\mu' r)^2}\right)\frac{e^{-\mu' r}}{\mu' r} - \left(\frac{\alpha}{\mu}\right)^3\left(1+\frac{3}{\alpha r}+\frac{3}{(\alpha r)^2}\right)\frac{e^{-\alpha r}}{\alpha r}\right\}. \tag{2-27}$$

For pion kinetic energies in excess of roughly 180 MeV, we find that $q^2 > 3\mu^2$, or $\mu'^2 < 0$. In this case, the contour integrals are obtained by raising the positive real pole slightly above the real axis while the negative real pole is lowered. The general results are then given by

$$f_{n\ell}(r) = -i\left(\frac{|\mu'|}{\mu}\right)^{n-1}\frac{1}{2}\left\{h_\ell'(|\mu'|r) + (-1)^n h_\ell^2(-|\mu'|r)\right\}$$

and

$$\tilde{f}_{n\ell}(r) = -\left(\frac{\alpha^2+\beta^2}{\alpha^2-\mu'^2}\right)\left\{ i\left(\frac{|\mu'|}{\mu}\right)^{n-1}\frac{1}{2}\left\{h_\ell'(|\mu'|r) + (-1)^n h_\ell^2(-|\mu'|r)\right\}\right.$$
$$\left. - i^n\left(\frac{\alpha}{\mu}\right)^{n-1}\frac{1}{2}\left\{h_\ell'(i\alpha r) + (-1)^n h_\ell^2(-i\alpha r)\right\}\right\}.$$

(2-28)

Explicit expressions analogous to those of Eq. (2-27) are easily obtained. The contribution from the pole, μ', in this case reflects an outgoing spherical wave.

We turn now to some exploratory calculations below the resonance and present results obtained using various terms in the Hamiltonian interaction density. At low pion energies, the dimensionless scattering parameters, λ_i, may be determined from results given by Klein. The subscript, 2, indicates evaluation in the two-body (pi-nucleon) frame. The N-star term in the p-wave scattering is neglected to obtain

$$\lambda_1 = -\frac{1}{6}\frac{\mu}{g_2}(\delta_1 + 2\delta_3),$$
$$\lambda_2 = \frac{1}{6}\frac{\mu}{g_{20}}\frac{\mu}{g_2}(\delta_1 - \delta_3),$$
$$\lambda_3 = -\left(\frac{\mu}{g_2}\right)^3(\delta_{33} + \frac{1}{2}\delta_{13})$$

and

$$\lambda_4 = \frac{1}{2}\left(\frac{\mu}{g_2}\right)^3(\delta_{33} - \delta_{13}).$$

(2-29)

In writing these equations, use has been made of the approximation, $\delta \sim \sin \delta$. The s-wave phase shifts are designated δ_{2t}, while the p-wave phase shifts are given by $\delta_{2t,2j}$. For these first calculations, the scattering parameters are not taken to be energy-dependent, but are instead evaluated near zero energy. With the phase shift parameterization of McKinley,[81] the parameters, λ_i, are 0.0054, 0.0445, -0.2407 and 0.1230. However, the energy-dependent results do not change significantly in the first 100 MeV.

Figure 4 presents results using various terms in the Hamiltonian. These calculations were performed over a pion kinetic energy range from 2 to 100 MeV using the Hamada-Johnston potential for initial and final nucleon-nucleon states. The experimental data in Fig. 4 are obtained from references 62, 64-72 and 102.

In the first calculation, only direct absorption processes involving the transition operator, T^0, are considered. As shown in Fig. 4, the direct absorption result tends nearly to vanish at low energy. This is a consequence of the accidental cancellation of the s-wave absorption operator terms from S- and D-states of the deuteron. This effect has been previously noted by several authors.[44,45,49] The contribution from the p-wave absorption operator, on the other hand, can easily be shown proportional to the incident pion momentum. This is the behavior exhibited by the first curve in Fig. 4.

Addition of the s-wave scattering terms of Eq. (2-3) produces the q^{-1} behavior which characterizes the low-energy experimental data. This result is shown clearly in Fig. 4. At 2 MeV, a comparison may be made directly with the bound-state calculation of Koltun and Reitan. Six of the integrals in Eq. (2-23), when performed with the $^3S_1$ and $^3D_1$ initial

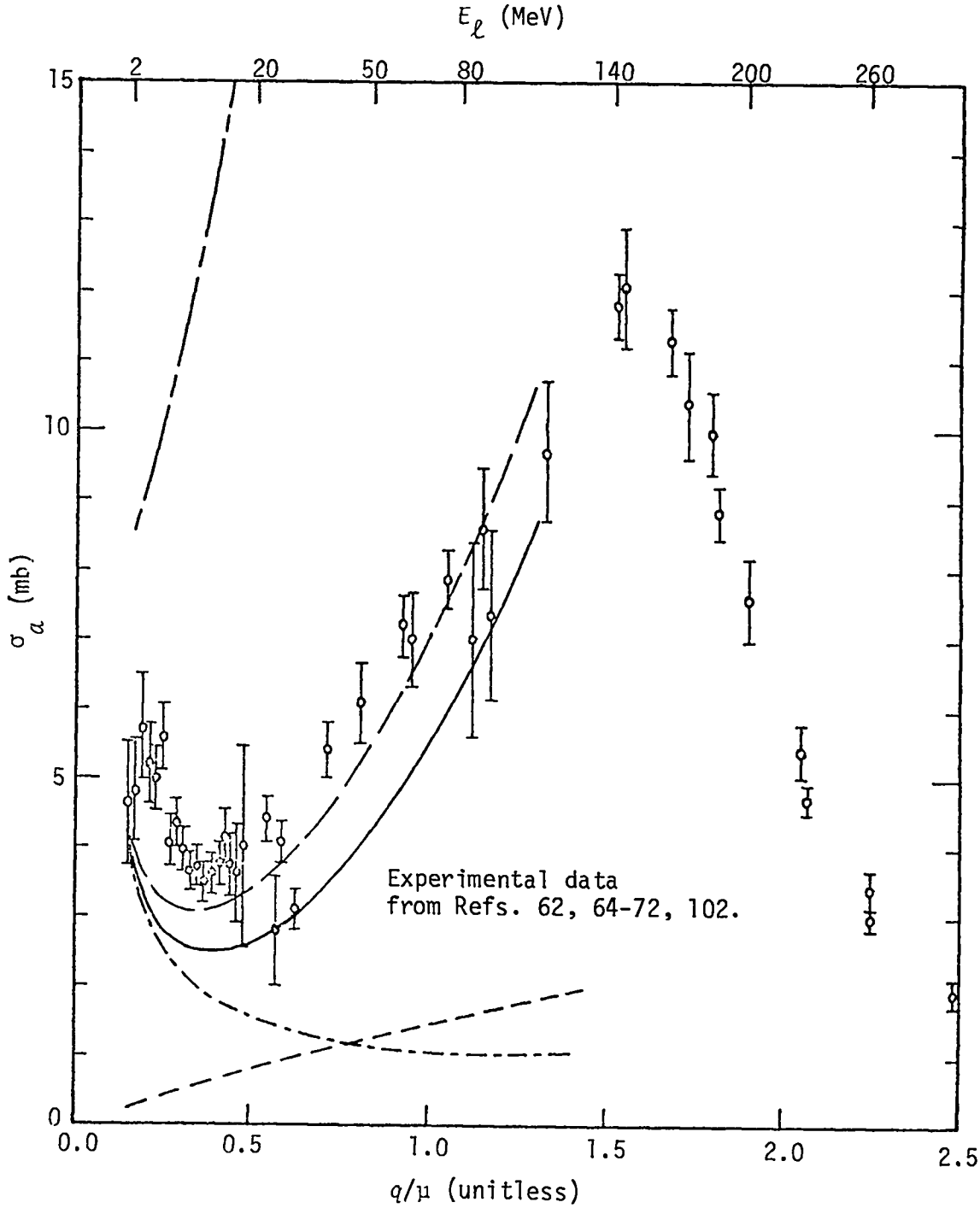

Fig. 4. Cross sections for various Hamiltonian terms.

- – – – – direct absorption only
- – – – – direct absorption and s-wave scattering
- – ——— full calculation with Klein p-wave
- ——— full calculation with on-shell p-wave
- ——— ——— above, with Galilean invariance omitted

and $^3P_1$ final states, differ in form from their integrals only by the factor, $j_0(\frac{qr}{2})$. This factor is nearly unity for small pion momentum, so that numerical agreement to within two percent is obtained for all six comparable integrals. No p-wave scattering is considered in this calculation, and as the result in Fig. 4 shows, there is clearly no hope of reproducing the experimental absorption resonance with s-wave scattering processes.

Next, the Klein p-wave scattering terms given in Eq. (2-4) are added to the calculation. Equivalently, the separable forms in Eq. (2-5) may be used with a value of infinity for α. In this case we have for the intermediate integrals, $\tilde{f}_{n\ell} \to f_{n\ell}$. Inclusion of the Klein p-wave terms leads to the excessively large result shown in Fig. 4. This result would seem to reflect the divergent nature of the intermediate integrals, in particular, f_{42}.

By evaluating these integrals numerically, it is possible to introduce a cutoff in the intermediate pion momentum. Use of a cutoff in the Klein p-wave terms is found to improve substantially the agreement with experiment; however, the calculation is extremely sensitive to the cutoff value chosen. This simply reflects the divergent nature of the critical integrals.

Several alternatives to a sharp momentum cutoff are possible. First, it is apparent that a simple reduction in the power of q' in the p-wave intermediate integrals will have a beneficial effect. This idea suggests that useful forms for the p-wave scattering Hamiltonians might be

$$H_{ij}^{3} = -4\pi\lambda_3\mu^{-3}q^2(\hat{q}_\pi\phi_i)\cdot(\hat{q}_\pi\phi_j)$$

and

$$H_{ij}^{4} = -4\pi\lambda_4\mu^{-3}q^2\bar{\sigma}_i\gamma_i\cdot(\hat{q}_\pi\phi_i)\times(\hat{q}_\pi\phi_j) \quad . \tag{2-30}$$

These forms have the property of kinematical equivalence at low energy to the on-shell free scattering amplitudes. For this reason, we will refer to Eq. (2-30) as the on-shell Hamiltonian. It will be seen that the angular properties of Eq. (2-5) are unchanged; thus the essential replacements in Eq. (2-23) are simply

$$\tilde{f}_{31}(r) \longrightarrow \frac{q}{\mu} f_{21}(r),$$
$$\tilde{f}_{40}(r) \longrightarrow \frac{q}{\mu} f_{30}(r)$$

and

$$\tilde{f}_{42}(r) \longrightarrow \frac{q}{\mu} f_{32}(r) \quad . \tag{2-31}$$

The result using the on-shell p-wave Hamiltonian of Eq. (2-30) is shown by the solid curve in Fig. 4. This curve is seen to reasonably represent the experimental data. This result bears some similarity to that presented by Reitan,[48] who extended his previous calculation to 20 MeV pion kinetic energy with new scattering parameters to obtain better agreement with the data of Rose. Reitan's p-wave scattering Hamiltonians are believed similar to those of Eq. (2-30).[82]

We present one other calculation of interest using the on-shell p-wave Hamiltonian. Following a suggestion by Miller,[83] we delete the

s-wave operator from the direct absorption term, H^0. Certain integrals in Eq. (2-23) are therefore omitted and kinematical corrections are made to those remaining. The calculation is now frame dependent; the result shown in Fig. 4 is obtained in the overall-center-of-mass frame. Again, the small difference between this result and that preceding it reflects the cancellation of the direct s-wave terms. However, the main point is that the calculated cross section for this reaction is relatively insensitive to the presence of the Galilean-invariant term.

Although the p-wave Hamiltonian terms given in Eq. (2-30) are reasonably successful in reproducing the experimental data, this result would not seem to have a firm theoretical basis. First, in the low-energy limit, these forms do not reduce to Klein's results given in Eq. (2-4). It also seems reasonable to require that the Hamiltonian vanish far off-shell, while for the forms in question, the off-shell and on-shell properties are the same and constant.

We turn now to the p-wave scattering Hamiltonian suggested in Eq. (2-5). These terms were created expressly to satisfy the requirements stated above. In this approach, α is treated as a free parameter. To permit calculation through the absorption resonance region, the scattering parameters, λ_i, are taken to be complex and are determined according to results presented in Appendix VIII rather than those given in Eq. (2-29).

Figure 5 presents results for calculations performed with the full Hamiltonian, including the p-wave terms of Eq. (2-5). These results were obtained using the Hamada-Johnston potential for initial and final nuclear states, and three different values of the off-shell paramater, α. As can be seen, the calculation shows great sensitivity to this parameter.

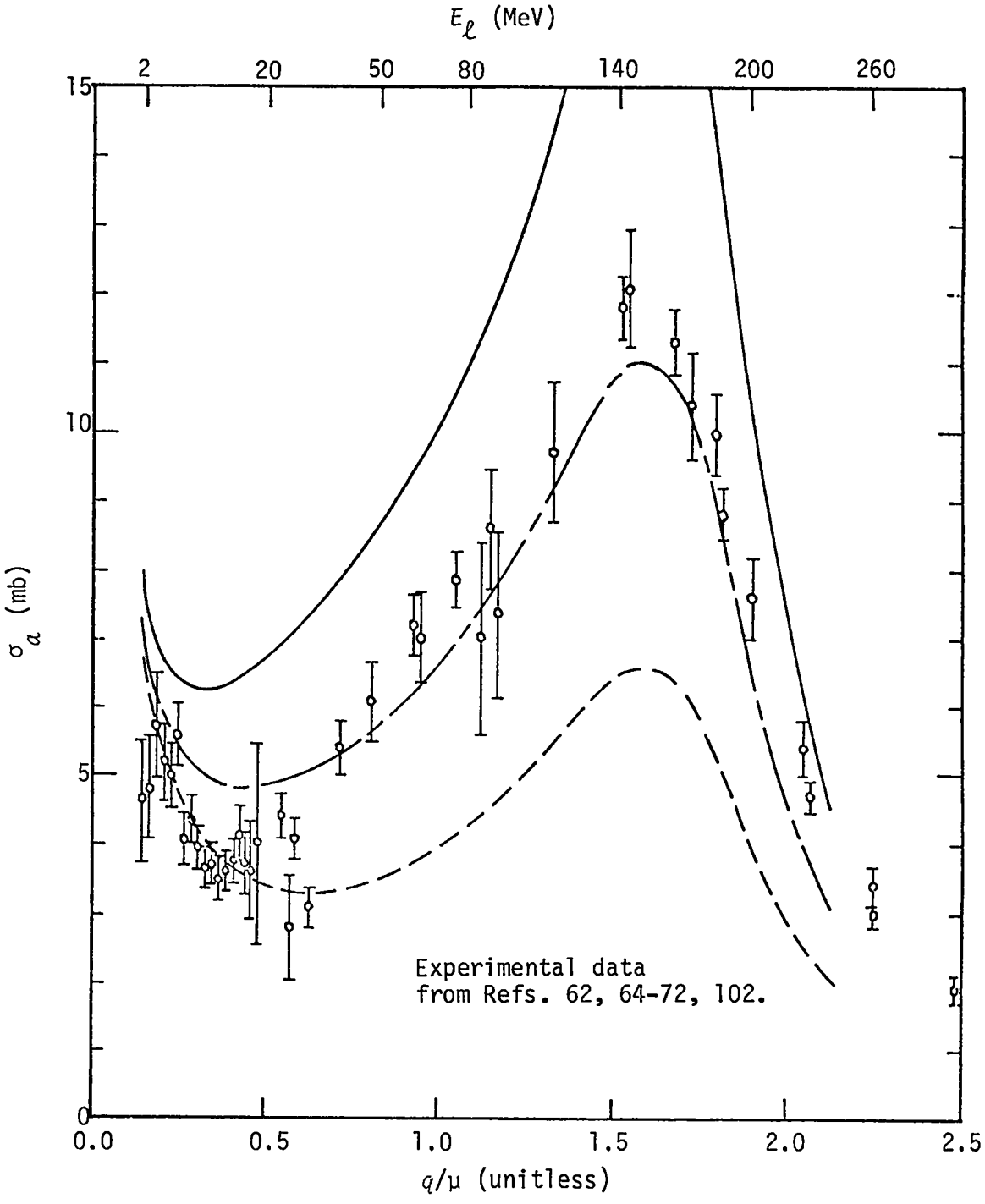

Fig. 5. Cross sections for the separable Hamiltonian and Hamada-Johnston wave functions.

– – – – – α = 200 MeV/c
– ——— – α = 300 MeV/c
——————— α = 400 MeV/c

A similar set of curves is shown in Fig. 6 for the Boundary Condition Model with 7.55% D-state in the deuteron. These results are seen to be very similar to those obtained with the Hamada-Johnston potential, and exhibit the same degree of sensitivity to the off-shell behavior. The fourth curve in Fig. 6 was obtained using the value, α = 300 MeV/c, and the Boundary Condition Model with 4.60% D-state in the deuteron.

As can be seen from Figs. 5 and 6, a value of α slightly in excess of 300 MeV/c seems likely to produce a reasonable fit to the experimental data. Previous estimates of this parameter have included 230,[78] 336[77] and 519[76] MeV/c. Thus this calculation would seem extraordinarily sensitive to the off-shell parameter.

It is not difficult to see why this process is so sensitive to the off-shell character of pi-nucleon scattering. If the initial and final states of the nucleons are taken to be on-shell, then the intermediate pion must propagate with an energy, $q_0/2$ (the external pion must give half its energy to each nucleon). The intermediate momentum is then given by

$$q'^2 = \frac{q^2}{4} - \frac{3\mu^2}{4} . \qquad (2\text{-}32)$$

Thus knowledge of the behavior of both the absorption and scattering vertices is required far off-shell. It is assumed that Eq. (2-2) represents the absorption vertex correctly, although at higher pion momenta this can be questioned. But the essential point is that the off-shell momentum enters the matrix element through both vertices.

We turn now to angular distributions calculated using the value, α = 300 MeV/c. Results in the following figures present comparisons

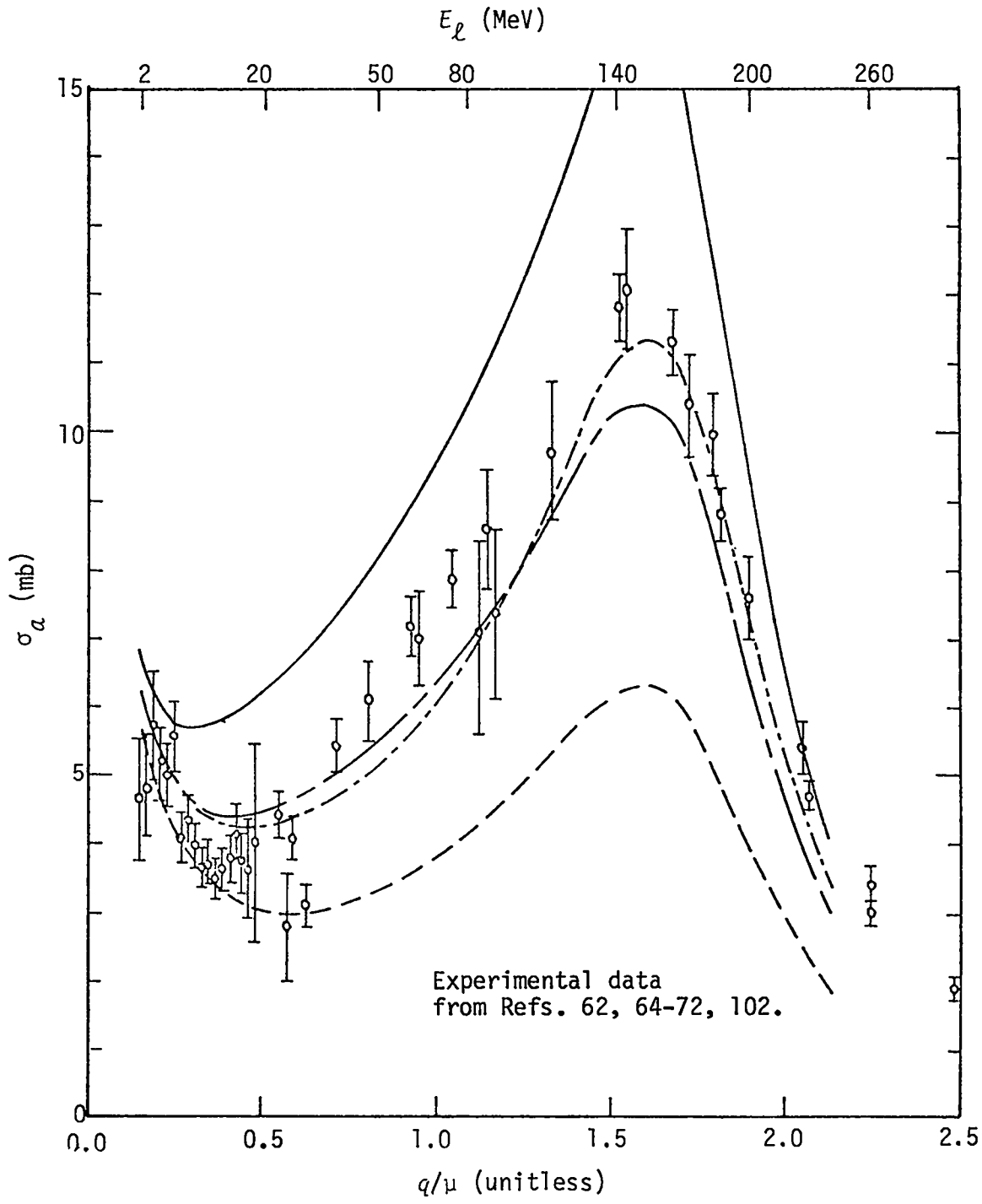

Fig. 6. Cross sections for the separable Hamiltonian and Boundary Condition Model wave functions.

- – – – – α = 200 MeV/c, 7.55% D-state
- – ——— – α = 300 MeV/c, 7.55% D-state
- ——————— α = 400 MeV/c, 7.55% D-state
- — · — · — α = 300 MeV/c, 4.60% D-state

for the three different nucleon-nucleon potentials. For the low-energy data, we follow precedent and plot the ratio of the two leading coefficients of Eq. (2-16) vs incident pion momentum. These results are compared in Fig. 7 with an experimental data compilation by Rosenfeld.[63] We note that only the coefficients, C_0 and C_2, enter our calculated ratio. On the other hand, the experimentally determined ratios are probably the result of forcing the data to a degree-two fit, and may thus include higher-order terms. Therefore, use of this ratio may be misleading, and we would prefer comparison directly with the cross section measurements.

In Fig. 7, the Boundary Condition Model with 7.55% D-state is seen to give similar results to the Hamada-Johnston, which has a 7.00% D-state. The 4.60% D-state BCM case lies considerably above the other two, thereby implying a possible sensitivity to the fraction of D-state in the deuteron. The previously mentioned experiment at LAMPF is designed for accuracy sufficient, in principle, to permit selection of a preferred nuclear model.

For higher energies, we follow the usual convention of plotting the differential cross section vs $\cos^2\theta$. These results are compared with experimental data at six pion kinetic energies in Figs. 8 and 9. The calculated results are seen to give reasonable agreement with experiment, particularly below and near the resonance.

Above the resonance, there is experimental evidence for negative coefficients in the higher powers of $\cos^2\theta$. It should be pointed out that this calculation has neglected multiple-scattering graphs as well as the nonunitarity of the proton-proton wave functions. This absorption

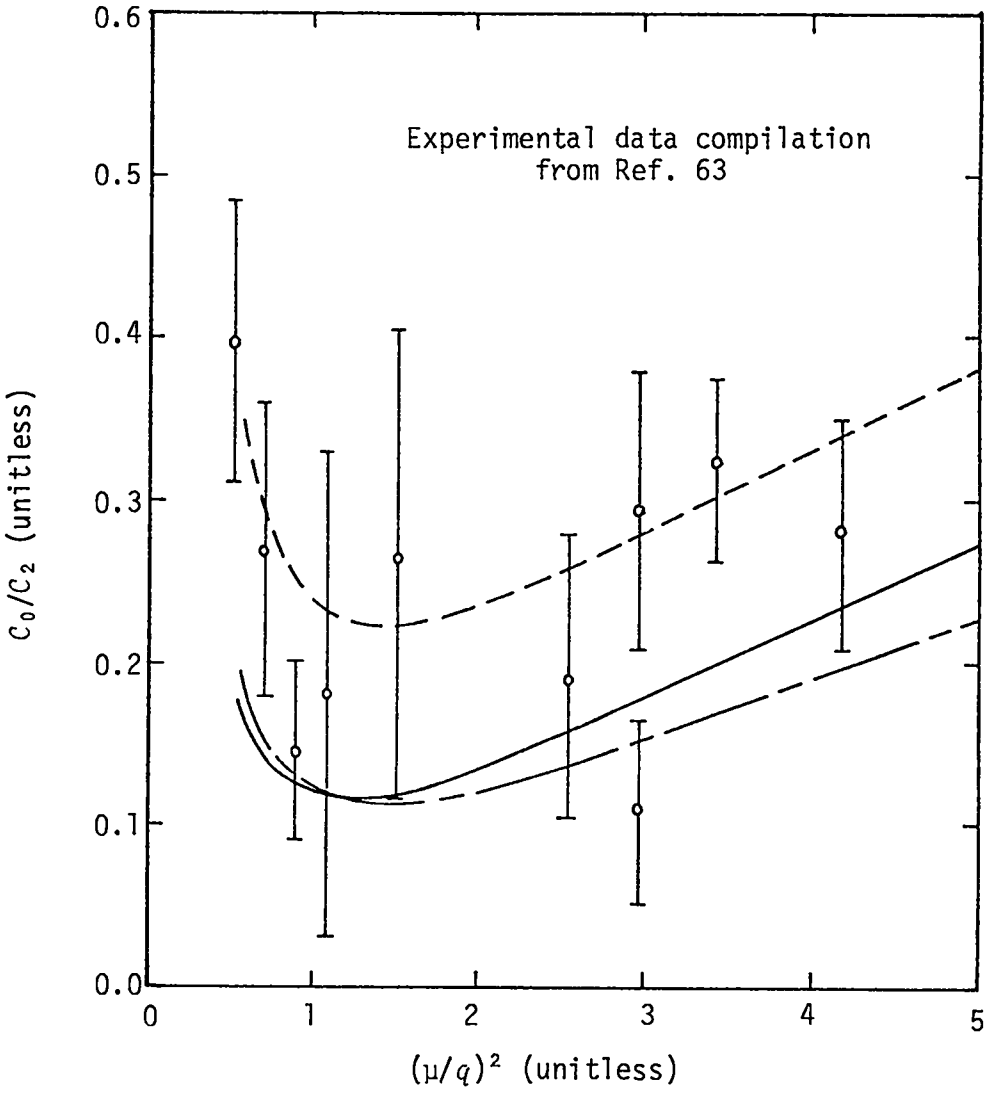

Fig. 7. Differential cross section coefficients for the separable Hamiltonian with α = 300 MeV/c.

– – – – – Boundary Condition Model with 4.60% D-state

– ——— – Boundary Condition Model with 7.55% D-state

——————— Hamada-Johnston potential with 7.00% D-state